



Deposited via The University of York.

White Rose Research Online URL for this paper:

<https://eprints.whiterose.ac.uk/id/eprint/3692/>

---

**Article:**

Song, L-Y., de Lamare, R.C. and Burr, A.G. (2008) Successive interference cancellation schemes for time-reversal space-time block codes. *IEEE Transactions on Vehicular Technology*. pp. 642-648. ISSN: 0018-9545

<https://doi.org/10.1109/TVT.2007.905602>

---

**Reuse**

Items deposited in White Rose Research Online are protected by copyright, with all rights reserved unless indicated otherwise. They may be downloaded and/or printed for private study, or other acts as permitted by national copyright laws. The publisher or other rights holders may allow further reproduction and re-use of the full text version. This is indicated by the licence information on the White Rose Research Online record for the item.

**Takedown**

If you consider content in White Rose Research Online to be in breach of UK law, please notify us by emailing [eprints@whiterose.ac.uk](mailto:eprints@whiterose.ac.uk) including the URL of the record and the reason for the withdrawal request.

*promoting access to White Rose research papers*



**Universities of Leeds, Sheffield and York**  
**<http://eprints.whiterose.ac.uk/>**

---

White Rose Research Online URL for this paper:  
<http://eprints.whiterose.ac.uk/3692/>

---

**Published paper**

Song, L.Y., de Lamare, R.C. and Burr, A.G. (2008) *Successive interference cancellation schemes for time-reversal space-time block codes*, IEEE Transactions on Vehicular Technology, Volume 57 (1), 642 - 648.

---

## Successive Interference Cancellation Schemes for Time-Reversal Space-Time Block Codes

Lingyang Song, *Student Member, IEEE*,  
Rodrigo C. de Lamare, *Member, IEEE*, and  
Alister G. Burr, *Member, IEEE*

**Abstract**—In this paper, we propose two simple signal detectors that are based on successive interference cancellation (SIC) for time-reversal space-time block codes to combat intersymbol interference in frequency-selective fading environments. The main idea is to treat undetected symbols and noise together as Gaussian noise with matching mean and variance and use the already-detected symbols to help current signal recovery. The first scheme is a simple SIC signal detector whose ordering is based on the channel powers. The second proposed SIC scheme, which is denoted parallel arbitrated SIC (PA-SIC), is a structure that concatenates in parallel a certain number of SIC detectors with different ordering sequences and then combines the soft output of each individual SIC to achieve performance gains. For the proposed PA-SIC, we describe the optimal ordering algorithm as a combinatorial problem and present a low-complexity ordering technique for signal decoding. Simulations show that the new schemes can provide a performance that is very close to maximum-likelihood sequence estimation (MLSE) decoding under time-invariant conditions. Results for frequency-selective and doubly selective fading channels show that the proposed schemes significantly outperform the conventional minimum mean square error-(MMSE) like receiver and that the new PA-SIC performs much better than the proposed conventional SIC and is not far in performance from the MLSE. The computational complexity of the SIC algorithms is only linear with the number of transmit antennas and transmission rates, which is very close to the MMSE and much lower than the MLSE. The PA-SIC also has a complexity that is linear with the number of SIC components that are in parallel, and the optimum tradeoff between performance and complexity can be easily determined according to the number of SIC detectors.

**Index Terms**—Equalization, frequency-selective fading, successive interference cancellation (SIC), time-reversal space-time block codes (TR-STBCs).

### I. INTRODUCTION

A number of researchers have pointed out the substantial capacity advantages that are available in wireless systems using multiple receive/transmit antennas [known as “multiple-in–multiple-out” (MIMO) channels]. This has led to the development of Lucent’s “Bell-Labs layered space-time” (BLAST) architecture [1]–[4] and space-time block codes (STBCs) [5]–[7] to achieve some of this capacity. STBCs can provide maximum diversity gain, aiming at improving communication quality and robustness. A simple transmit diversity scheme for two transmit antennas was first proposed by Alamouti [5] to improve the quality and the data rate in wireless communication systems. As a further extension to more than two transmit antennas, orthogonal STBCs were later reported in [6] and [7]. The popularity of STBCs stems from their ability to offer maximum-likelihood (ML) decoding with simple linear processing at the receiver side. Also, unlike MIMO schemes based on BLAST, STBCs can utilize any number of receive antennas, thus simplifying the mobile terminal design. How-

ever, STBCs, as proposed in [5]–[7], assume frequency-flat channels and suffer performance degradation over frequency-selective channels.

Recently, space-time coding for frequency-selective fading environments has attracted great attention, and it has been demonstrated that the downlink performance of wireless communication systems can be significantly improved by properly designed burst-based STBCs. Methods such as time reversal [8], orthogonal frequency division multiplexing (OFDM) [9], [10], and single-carrier frequency-domain equalization [11]–[13] can be combined to combat ISI. More recently, in [14], several transmission schemes and decoding algorithms have been reported for time-reversal space-time block codes (TR-STBCs). However, the above techniques for the frequency-selective environment, by combining STBCs with other schemes, do not fully make use of the properties that orthogonal coding structures have in the time domain. Space-frequency OFDM may not fully exploit frequency diversity [9], [10] if no outer codes are used; the realization of frequency diversity using OFDM only is of great interest. In [8] and [14], it was shown that optimal performance is difficult to obtain due to equalizer limitations.

In this paper, we propose a very simple signal detector that is based on successive interference cancellation (SIC) for the TR-STBCs to combat ISI in dispersive fading channels. The main idea is to subtract the effect of the already-detected signals from the received signals and treat undetected symbols and noise together as Gaussian noise with matching mean and variance by Gaussian approximation [15], [16], such that the resulting signal detector has very low computational complexity. Simulation results show that our scheme can provide a bit error rate (BER) that is very close to ML sequence estimation (MLSE) decoding under time-invariant conditions. Note that in [17], ordered SIC was proposed to decode the vertical BLAST system. The major difference in our proposed SIC is that we consider the covariance of the undetected signals and its corresponding channel information.

Although for frequency-selective and time-selective (doubly selective) fading channels our SIC detector can outperform the conventional MMSE-like receiver, there exists a gap when the SIC detector is compared to the MLSE decoder. To this end, we further parallel-concatenate a certain number of SIC detectors with different signal decoding sequences. Instead of making hard decisions, each SIC detector produces soft output, which is then combined for final detection—a process that we term “parallel arbitrated SIC” (PA-SIC). Simulation shows that the PA-SIC can provide much better performance than the SIC. Performance and complexity can be traded off by choosing the number of SIC branches.

In [18], a related PA-SIC was proposed for multiuser detection. Our proposed PA-SIC differs from it in several respects. First, our SIC component is based on a Gaussian approximation, which is potentially different from the SIC used in [18], which applies the matched filter and does not consider the joint effects of undetected terms and the noise. Second, the parallel search in [18] depends on randomly choosing a certain number of branches with different signal detection sequences; however, in our PA-SIC, the sequence that is arranged by decreasing power signal ordering (DP-SO) must be included, and furthermore, in later simulations, we show that the SIC with DP-SO can provide better performance than the SIC that is based on symbol arrival instant SO (SAI-SO), which means that the SIC with DP-SO can realize a more reliable estimate. Last, the output of the SIC branches can be combined for joint signal recovery, whereas the PA-SIC in [18] only selects the branch with the most reliable estimates.

The rest of this paper is organized as follows. In Section II, we introduce some preliminaries including the channel and system model and the TR-STBCs. The SIC and the PA-SIC are described in Section III.

Manuscript received October 16, 2006; revised March 7, 2007, May 8, 2007, and June 4, 2007. The review of this paper was coordinated by Dr. A. Ghayeb.

L. Song is with UniK—University Graduate Center, University of Oslo, 2027 Kjeller, Norway (e-mail: lingyang@unik.no).

R. C. de Lamare and A. G. Burr are with the Communications Research Group, Department of Electronics, University of York, YO10 5DD York, U.K. (e-mail: rcd1500@ohm.york.ac.uk; alister@ohm.york.ac.uk).

Color versions of one or more of the figures in this paper are available online at <http://ieeexplore.ieee.org>.

Digital Object Identifier 10.1109/TVT.2007.905602

Simulation results are shown in Section IV. In Section V, our main conclusions are given.

## II. PRELIMINARIES

### A. System and Channel Model

The frequency-selective channel can be modeled using a finite-impulse response (FIR) filter with maximum time delay  $L$ , i.e.,

$$H_i(n) = \sum_{k=1}^L h_i(k)\delta(n-k) \quad (1)$$

where  $i$  denotes the  $i$ th transmit antenna, and  $L$  is the length of the FIR filter. The FIR filter coefficients are normalized to  $\sum_{i=1}^{N_T} \sum_{k=1}^L |h_i(k)|^2 = N_T$ , and  $N_T$  denotes the number of transmit antennas. The received signals can be written as follows:

$$r(n) = \sum_{i=1}^{N_T} H_i(n) * s_i(n) + n(n) \quad (2)$$

where  $s_i(n)$  stands for the transmitted signal,  $*$  denotes the discrete-time convolution, and  $n(n)$  denotes the independent samples of a zero-mean complex Gaussian random variable with variance  $\sigma^2 = E/(2\text{SNR})$ .  $E$  denotes the total power of transmitted signals.

Provided that only two transmit antennas are used, (2) can be rewritten as follows:

$$\mathbf{r} = \mathbf{H}\mathbf{s} + \mathbf{n} \quad (3)$$

where the received signals have length  $N + L - 1$ ,  $\mathbf{r} = [r(1), \dots, r(N + L - 1)]^T$ , transmitted signals  $\mathbf{s} = [s_1(1), \dots, s_1(N), s_2(1), \dots, s_2(N)]^T$ , and  $\mathbf{n} = [n(1), \dots, n(N)]^T$ . The time-domain presentation of  $\mathbf{H}$  with dimension  $(N + L - 1) \times (2N)$  is shown at the bottom of the page.

Let  $\mathbf{H} = (\mathbf{H}_1 \quad \mathbf{H}_2)$ , where  $\mathbf{H}_i$  is the channel expression for the  $i$ th transmit antenna with size  $(N + L - 1) \times N$ . Note that this system and transmission scheme can be easily extended to configurations with more transmit antennas. For the sake of simplicity, we will focus on the case of two transmit antennas in this paper.

### B. LS Channel Estimation

The received signals in (3) can be written in the form of a training sequence  $\mathbf{S}$  and an instantaneous channel response  $\mathbf{h}$ , i.e.,

$$\mathbf{r} = \mathbf{S}\mathbf{h} + \mathbf{n}$$

where  $\mathbf{h} = (h_1(0), \dots, h_2(L-1), h_2(0), \dots, h_2(L-1))^T$ . By considering the least squares (LS) cost function  $J = \sum \|\mathbf{S}\mathbf{h} - \mathbf{r}\|^2$ , we

calculate its gradient with respect to  $\mathbf{h}$  and set it to a null vector  $\mathbf{0}$ . Hence, the LS channel estimator can be expressed as follows:

$$\mathbf{h} = (\mathbf{S}^H \mathbf{S})^{-1} \mathbf{S}^H \mathbf{r} \quad (4)$$

### C. TR-STBCs

The TR-STBCs extend STBCs for transmission over frequency-selective channels by encoding together conventionally ordered and time-reversed contiguous blocks of symbols [8], [14]. In this section, we briefly describe the TR-STBCs. For simplicity, we only consider a system with two transmit antennas and one receive antenna operating in a frequency-selective fading environment.

At the transmitter end, the modulated vector  $\mathbf{s}$ , which has length  $2N$ , is split into two contiguous subblocks  $\mathbf{s}_1$  and  $\mathbf{s}_2$ , each of which is of length  $N$ . Each block is divided into two halves or subblock periods. During the first subblock period,  $\mathbf{s}_1$  will be transmitted from the first antenna, while  $\mathbf{s}_2$  will be simultaneously sent from the second antenna. The corresponding received signals can be represented as follows:

$$\mathbf{r}_1 = \mathbf{H}_1 \mathbf{s}_1 + \mathbf{H}_2 \mathbf{s}_2 + \mathbf{n}_1 \quad (5)$$

where  $\mathbf{r}_1$  is the received vector of  $N$  samples,  $\mathbf{H}_i$  is the time-domain representation of the channels, and  $\mathbf{n}_1$  is the noise. In the second subblock period,  $\mathbf{s}_2$  is time reversed, complex conjugated, negated, denoted as  $-\bar{\mathbf{s}}_2^*$ , and then transmitted from the first antenna; at the same time,  $\mathbf{s}_1$  is time reversed and complex conjugated, and  $\bar{\mathbf{s}}_1^*$  is transmitted from the second antenna. Then, we can obtain

$$\bar{\mathbf{r}}_2 = -\mathbf{H}_3 \bar{\mathbf{s}}_2^* + \mathbf{H}_4 \bar{\mathbf{s}}_1^* + \bar{\mathbf{n}}_2. \quad (6)$$

1) *Frequency-Selective and Time-Invariant Fading Channels*: In frequency-selective but time-invariant conditions, we have  $\mathbf{H}_1 = \mathbf{H}_3$  and  $\mathbf{H}_2 = \mathbf{H}_4$ . We can rewrite (6) as follows:

$$\mathbf{r}_2 = -\bar{\mathbf{H}}_1^* \mathbf{s}_2 + \bar{\mathbf{H}}_2^* \mathbf{s}_1 + \mathbf{n}_2 \quad (7)$$

where  $\bar{\mathbf{H}}_i$  is the time-reversed expression of  $\mathbf{H}_i$ . It should be noted that some form of guard interval is necessary to avoid interblock interference between the received signals. We can now further reach the following:

$$\underbrace{\begin{pmatrix} \mathbf{r}_1 \\ \mathbf{r}_2 \end{pmatrix}}_{\mathbf{r}} = \underbrace{\begin{pmatrix} \mathbf{H}_1 & \mathbf{H}_2 \\ \bar{\mathbf{H}}_2^* & -\bar{\mathbf{H}}_1^* \end{pmatrix}}_{\mathbf{H}} \underbrace{\begin{pmatrix} \mathbf{s}_1 \\ \mathbf{s}_2 \end{pmatrix}}_{\mathbf{s}} + \underbrace{\begin{pmatrix} \mathbf{n}_1 \\ \mathbf{n}_2 \end{pmatrix}}_{\mathbf{n}}. \quad (8)$$

At the receiver, a spatiotemporal matched filter  $\mathbf{H}^H$  is applied, i.e.,

$$\mathbf{y} = \mathbf{H}^H \mathbf{r} = \mathbf{H}^H \mathbf{H} \mathbf{s} + \mathbf{H}^H \mathbf{n} \quad (9)$$

$$\mathbf{H} = \begin{pmatrix} h_1(0) & 0 & \dots & 0 & h_2(0) & 0 & \dots & 0 \\ h_1(1) & h_1(0) & \dots & \vdots & h_2(1) & h_2(0) & \dots & \vdots \\ \vdots & h_1(1) & \dots & 0 & \vdots & h_2(1) & \dots & 0 \\ h_1(L-1) & \vdots & \dots & h_1(L-1) & h_2(L-1) & \vdots & \dots & h_2(L-1) \\ 0 & h_1(L-1) & \dots & h_1(L-2) & 0 & h_2(L-1) & \dots & h_2(L-2) \\ \vdots & \vdots & \dots & \vdots & \vdots & \vdots & \dots & \vdots \\ 0 & 0 & \dots & h_1(0) & 0 & 0 & \dots & h_2(0) \end{pmatrix}$$

which perfectly decouples the decoding of  $\mathbf{s}_1$  and  $\mathbf{s}_2$ . Since all off-diagonal terms of  $\mathbf{H}^H \mathbf{H}$  are zero, we can obtain

$$\begin{aligned} \mathbf{H}^H \mathbf{H} &= \begin{pmatrix} \mathbf{H}_1^H \mathbf{H}_1 + \mathbf{H}_2^H \mathbf{H}_2 & 0 \\ 0 & \mathbf{H}_1^H \mathbf{H}_1 + \mathbf{H}_2^H \mathbf{H}_2 \end{pmatrix} \\ &= \begin{pmatrix} \mathbf{J}_1 & 0 \\ 0 & \mathbf{J}_1 \end{pmatrix} = \mathbf{J} \end{aligned}$$

where  $\mathbf{J}_1$  is an  $N \times N$  matrix, and the decoding of  $\mathbf{s}_1$  and  $\mathbf{s}_2$  can be fully uncorrelated.

2) *Frequency-Selective and Time-Variant Fading Channels (Doubly Selective Fading Channels)*: After combining (5) and (6), we have

$$\underbrace{\begin{pmatrix} \mathbf{r}_1 \\ \mathbf{r}_2 \end{pmatrix}}_{\mathbf{r}} = \underbrace{\begin{pmatrix} \mathbf{H}_1 & \mathbf{H}_2 \\ \mathbf{H}_4^* & -\mathbf{H}_3^* \end{pmatrix}}_{\mathbf{H}} \underbrace{\begin{pmatrix} \mathbf{s}_1 \\ \mathbf{s}_2 \end{pmatrix}}_{\mathbf{s}} + \underbrace{\begin{pmatrix} \mathbf{n}_1 \\ \mathbf{n}_2 \end{pmatrix}}_{\mathbf{n}}. \quad (10)$$

In this case, spatiotemporal matched filtering has to be directly implemented, i.e.,

$$\begin{aligned} \mathbf{y} &= \mathbf{H}^H \mathbf{r} \\ &= \begin{pmatrix} \mathbf{H}_1^H \mathbf{H}_1 + \mathbf{H}_4^H \mathbf{H}_4 & \mathbf{H}_1^H \mathbf{H}_2 - \mathbf{H}_4^H \mathbf{H}_3 \\ \mathbf{H}_2^H \mathbf{H}_1 - \mathbf{H}_3^H \mathbf{H}_4 & \mathbf{H}_2^H \mathbf{H}_2 + \mathbf{H}_3^H \mathbf{H}_3 \end{pmatrix} \begin{pmatrix} \mathbf{s}_1 \\ \mathbf{s}_2 \end{pmatrix} + \mathbf{H}^H \begin{pmatrix} \mathbf{n}_1 \\ \mathbf{n}_2 \end{pmatrix}. \end{aligned} \quad (11)$$

### III. SIGNAL DETECTION FOR THE TR-STBCS

The original proposal of the TR-STBCs [4] suggests a whitening filter followed by an MLSE decoder. Besides this,  $\mathbf{s}_1$  and  $\mathbf{s}_2$  can be also decoded in complex form using standard MMSE approaches. Now, we introduce the SIC and PA-SIC algorithms.

#### A. SIC-Based Signal Detectors

Since the received signals have different expressions, in this section, we introduce our signal detector for the TR-STBCs over frequency-selective and doubly selective fading channels separately.

1) *Frequency-Selective and Time-Invariant Fading Channels*: The received signals in (9) can be further written as follows:

$$\mathbf{y}_1 = \mathbf{J}_1 \mathbf{s}_1 + \tilde{\mathbf{n}}_1 \quad (12)$$

$$\mathbf{y}_2 = \mathbf{J}_1 \mathbf{s}_2 + \tilde{\mathbf{n}}_2. \quad (13)$$

Obviously,  $\mathbf{s}_1$  and  $\mathbf{s}_2$  can be separately decoded, which is the main advantage of the TR-STBCs.

2) *Frequency-Selective and Time-Variant (Doubly Selective) Fading Channels*: The received signals cannot be decoupled, and (11) can be further written as follows:

$$\mathbf{y} = \mathbf{J} \mathbf{s} + \tilde{\mathbf{n}}. \quad (14)$$

Since (12)–(14) have the same expression, in the following, we take (14) as an example to describe our SIC algorithm. Equation (14) can be rewritten as follows:

$$\mathbf{y} = \sum_{i=1}^{2N} \mathbf{j}_i s_i + \tilde{\mathbf{n}} \quad (15)$$

where  $\mathbf{j}_i$  stands for the  $i$ th column of  $\mathbf{J}$ . SIC detection can be performed as follows.

- 1) DP-SO: The signals that have relatively larger channel power should be decoded before the signals with smaller power. For convenience, suppose that the power ordering sequence

is  $\|\mathbf{j}_1\|^2 > \|\mathbf{j}_2\|^2 > \dots > \|\mathbf{j}_{2N}\|^2$ . Accordingly, we begin with the symbol with the highest channel power  $s_1$ . The other undetected terms  $\sum_{i=2}^{2N} \mathbf{j}_i s_i$  plus the noise vector  $\tilde{\mathbf{n}}$  are treated together as a new Gaussian variable with matching mean and variance such that (15) can be approximately expressed as follows:

$$\mathbf{y} \approx \mathbf{j}_1 s_1 + \boldsymbol{\eta}. \quad (16)$$

$\boldsymbol{\eta}$  represents a vector of zero-mean complex Gaussian random variables with variance  $\Lambda_1 = \mathbf{J}_{2,2N}^H \mathbf{J}_{2,2N} |\bar{s}|^2 + \sigma^2 \mathbf{H}^H \mathbf{H}$ , where  $|\bar{s}|^2$  represents the average power of the symbols in constellation  $M$ , and  $\mathbf{J}_{i,l} = [\mathbf{j}_i, \dots, \mathbf{j}_l]$ . Here,  $\boldsymbol{\eta}$  is treated as a zero-mean Gaussian variable so that the probability function  $p(\mathbf{y}|\mathbf{s}_1)$  can be expressed by a 1-D Gaussian distribution, i.e.,

$$p(\mathbf{y}|\mathbf{s}_1) = \exp\left(-(\mathbf{y} - \mathbf{j}_1 s_1)^H \Lambda_1^{-1} (\mathbf{y} - \mathbf{j}_1 s_1)\right).$$

All the possible modulated symbols that are related to  $\mathbf{s}_1$  can be examined by

$$\tilde{s}_1 = \arg \min_{s_1 \in M} |(\mathbf{y} - \mathbf{j}_1 s_1)^H \Lambda_1^{-1} (\mathbf{y} - \mathbf{j}_1 s_1)| \quad (17)$$

where  $\Lambda_1^{-1}$  can be greatly simplified by the matrix inversion lemma, as shown in the Appendix. As a result,  $s_1$  can be estimated by choosing the smallest value of (17). Note that the signal decoding sequence here is based on DP-SO rather than SAI, according to which the detected signal can be put into its corresponding position in the memory stack. Comparison of various decoding sequences will be made later over doubly selective channels. Note also that in relatively slow fading environments (frequency selective only),  $\|\mathbf{j}_1\|^2 \approx \|\mathbf{j}_2\|^2 \approx \dots \approx \|\mathbf{j}_{2N}\|^2$ , and SO becomes less important since the channel power corresponding to each transmitted signal remains almost the same.

- 2) In the second detection, the previously detected symbol  $\tilde{s}_1$  should be subtracted from the total received signals to reduce the inter-antenna interference, i.e.,

$$\mathbf{y} - \mathbf{j}_1 \tilde{s}_1 = \tilde{\mathbf{y}} = \mathbf{j}_2 s_2 + \sum_{i=3}^{2N} \mathbf{j}_i s_i + \tilde{\mathbf{n}}.$$

Similarly, we can obtain  $\Lambda_2 = \mathbf{J}_{3,2N}^H \mathbf{J}_{3,2N} |\bar{s}|^2 + \sigma^2 \mathbf{H}^H$ , and  $s_2$  can be recovered by

$$\tilde{s}_2 = \arg \min_{s_2 \in M} |(\tilde{\mathbf{y}} - \mathbf{j}_2 s_2)^H \Lambda_2^{-1} (\tilde{\mathbf{y}} - \mathbf{j}_2 s_2)|.$$

- 3) For the  $k$ th detection, the previously detected symbols, which are denoted by  $\tilde{s}_1, \dots, \tilde{s}_{k-1}$ , can be used to decode  $s_k$ , i.e.,

$$\mathbf{y} - \mathbf{J}_{1,k-1} \tilde{\mathbf{S}}_{1,k-1} = \tilde{\mathbf{y}} = \mathbf{j}_k s_k + \sum_{i=k+1}^{2N} \mathbf{j}_i s_i + \tilde{\mathbf{n}}$$

where  $\tilde{\mathbf{S}}_{1,k-1} = [\tilde{s}_1, \dots, \tilde{s}_{k-1}]^T$ . Again, the undetected terms should be treated as a Gaussian variable. The following equation can be applied to calculate the probabilities for  $s_k$ :

$$\tilde{s}_k = \arg \min_{s_k \in M} |(\tilde{\mathbf{y}} - \mathbf{j}_k s_k)^H \Lambda_k^{-1} (\tilde{\mathbf{y}} - \mathbf{j}_k s_k)| \quad (18)$$

where  $\Lambda_k = \mathbf{J}_{k+1,2N}^H \mathbf{J}_{k+1,2N} |\bar{s}|^2 + \sigma^2 \mathbf{H}^H$  can be similarly simplified. The same detection process will be repeated in each trial until the last.

Note that in the time-invariant case,  $\mathbf{s}_1$  and  $\mathbf{s}_2$  can be separately decoded, such that we can use the SIC for each  $\mathbf{s}_1$  and  $\mathbf{s}_2$ , respectively;

for time-variant environments,  $\mathbf{s}_1$  and  $\mathbf{s}_2$  are coupled such that they have to be detected as in (14). The disadvantage is the increase in complexity. The above SIC approach can be also readily extended to more than four transmit antennas by using the half-rate STBCs in [2] and [3], and we can also show that the computational complexity of the SIC is very low and close to the linear receiver, as will be explained later.

### B. PA-SIC Detectors

The SIC algorithm starts decoding according to a certain sequence that is obtained by SO, which is only optimal for a certain number of transmit symbols. Thus, it is worthwhile to employ a certain number of SIC detectors in parallel, each of which has different SOs simultaneously, and combine the soft information generated by each for enhanced performance. In other words, besides the DP-SO, other decoding sequences will be randomly generated.

Note that each SIC branch has a different decoding sequence, such that the soft output of the SIC needs to be reordered to the same sequence as that of the input before the soft information combination. Each SIC is independent and calculates the error probability of every input bit given “1” or “0,” and the output will be rearranged according to SAI. Provided that BPSK is used, the soft output of each SIC component given “1” can be written as follows:

$$P(d_k^i = 1 | \mathbf{r}, \mathbf{H}) = \exp \left\{ - (\tilde{\mathbf{y}} - \mathbf{j}_k^i M(d_k^i = 1))^H (\Lambda_k^i)^{-1} \right. \\ \left. \times (\tilde{\mathbf{y}} - \mathbf{j}_k^i M(d_k^i = 1)) \right\}.$$

Given “0”

$$P(d_k^i = 0 | \mathbf{r}, \mathbf{H}) = \exp \left\{ - (\tilde{\mathbf{y}} - \mathbf{j}_k^i M(d_k^i = 0))^H (\Lambda_k^i)^{-1} \right. \\ \left. \times (\tilde{\mathbf{y}} - \mathbf{j}_k^i M(d_k^i = 0)) \right\}$$

where  $M(\cdot)$  represents the corresponding constellation symbol selected by  $d_k^i$ . Last, the “soft combining” block collects probabilities from all the SIC detectors to calculate the log-likelihood ratio (LLR) of the input and output bits. The likelihood ratio of the data is given by the ratio of the sum of the probabilities of all SIC branches with “1” input in this section to those branches with a “0” input

$$u_k = \log \frac{\sum_{i=1}^K P(d_k^i = 1 | \mathbf{r}, \mathbf{H})}{\sum_{i=1}^K P(d_k^i = 0 | \mathbf{r}, \mathbf{H})} \\ = \log \frac{\sum_{i=1}^K \exp \left\{ - (\tilde{\mathbf{y}} - \mathbf{j}_k^i M(d_k^i = 1))^H (\Lambda_k^i)^{-1} (\tilde{\mathbf{y}} - \mathbf{j}_k^i M(d_k^i = 1)) \right\}}{\sum_{i=1}^K \exp \left\{ - (\tilde{\mathbf{y}} - \mathbf{j}_k^i M(d_k^i = 0))^H (\Lambda_k^i)^{-1} (\tilde{\mathbf{y}} - \mathbf{j}_k^i M(d_k^i = 0)) \right\}}$$

where  $K$  denotes the number of SIC branches, and the total number of SIC branches is  $(2N)!$ . The decisions of the information bits are based on the LLR, i.e.,

$$\tilde{d}_k^i = \begin{cases} 1, & \text{sgn}(u_k) \geq 0 \\ 0, & \text{sgn}(u_k) < 0 \end{cases}$$

where  $\text{sgn}(\cdot)$  is the signum function.

Note that since only symbol probability density is required in the PA-SIC, the soft output of each SIC component can be calculated in the same way as for the BPSK case if other modulation schemes are applied.

TABLE I  
COMPUTATIONAL COMPLEXITY OF VARIOUS SCHEMES FOR ONE CODING  
FRAME WITH LENGTH  $N$ ;  $L$  IS THE NUMBER OF TAPS;  
BPSK CONSTELLATIONS

Detector	Additions+ Multiplications
SIC	$\frac{18N^3 + 106N^2 + 5N - 6(L-4)}{6}$
PA-SIC	$K \left( \frac{18N^3 + 120N^2 - 5N - 6(L-4)}{6} \right)$
MMSE	$\frac{18N^3 + 102N^2 + (12L-17)N - 6(N-1)}{6}$
MLSE	$o(n^N)$

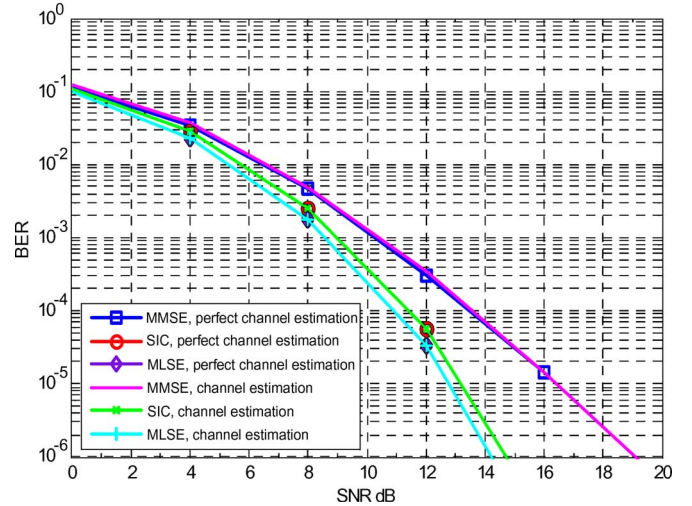


Fig. 1. SIC. Frequency-selective time-invariant fading channels; length of the frame = 64, taps = 3; BPSK. (a) Perfect channel estimation. (b) Channel estimation.

### C. Computational Complexity Analysis

In this section, we show the complexity of the SIC, PA-SIC, MMSE, and MLSE detectors in terms of the number of addition and multiplication operations. The resulting values are given in Table I, which are obtained by inspection of the relevant algorithms.

From the table, we observe that although the SIC slightly outperforms the MMSE, they are of the same complexity order  $o(n^3)$ . For the PA-SIC scheme, its complexity is proportional to the number of SIC branches, which can be obtained by the sum of the addition and multiplication operations of all the SIC detectors. The MLSE has the highest degree of complexity. Details of the computational complexity of matrix inversion can be found in [19]. As we can see from the table, the complexity of the SIC is very close to that of the minimum mean square error (MMSE), whereas that of the PA-SIC is about  $K$  times the complexity of the SIC, where  $K$  is the number of branches.

## IV. SIMULATION RESULTS

In all simulations, for simplicity, we consider only a system with two transmit antennas and one receive antenna, and BPSK and 16-quadrature amplitude modulation (16-QAM) constellations are used to generate a rate of 1- and 4-b/s/Hz transmission, respectively. Carrier frequency  $f_c = 2$  GHz, symbol period  $T_s = 128/(3.84 \times 10^6)$ , and Jakes' model are applied to construct a time-selective fading environment. The channel varies symbol by symbol, and perfect channel estimation is assumed at the receiver end. All the simulations are plotted with two vehicle speeds— $v = 0$  and 150 km/h (corresponding

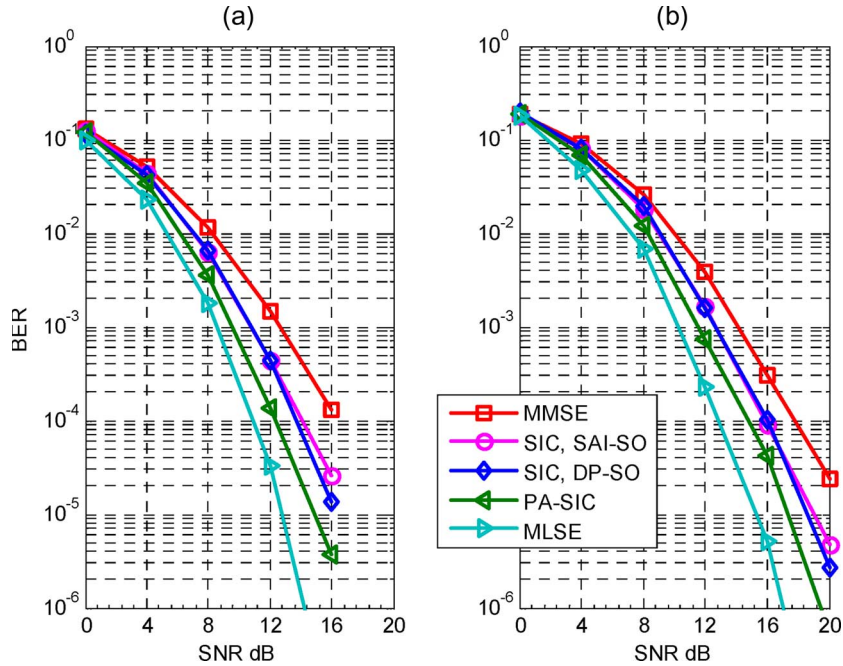


Fig. 2. SIC. Doubly selective fading channels; length of the frame = 64, taps = 3,  $k = 3$ ,  $F_d T_s = 0.0093$ ; BPSK. (a) Perfect channel estimation. (b) Channel estimation.

to  $f_d T_s = 0$  and 0.0093, respectively, where  $f_d = v f_c / c$ , and  $c$  is the speed of light).

In Fig. 1, simulation results for the SIC detector are illustrated in comparison with those of the conventional MMSE and the optimal MLSE decoder. Performance is determined over frequency-selective time-invariant fading channels. As shown in (12) and (13), the decoding of  $s_1$  and  $s_2$  can be separated, and thus, the SIC algorithm can be applied to recover  $s_1$  and  $s_2$ , respectively. From the figure, it can be observed that at  $\text{BER} = 10^{-4}$ , the performance is 4 dB better than that of the MMSE equalizer, and there is only 0.5-dB loss as compared to that of the MLSE decoder. We can achieve that performance in a relatively slow fading environment, where the SIC detector is able to provide near-optimal performance with much lower computational complexity. Since channel estimation is accurate enough, we can observe from Fig. 1 that there is almost no difference between the curves that are obtained with the channel estimation and those with perfect channel knowledge at the receiver.

Fig. 2 shows the simulation results in doubly selective fading channels. From the simulation results with perfect channel estimation in Fig. 2(a), we can see that the SIC with SAI-SO can obtain about 2-dB gain over the MMSE at  $\text{BER} = 10^{-4}$ . The power ordering is useful. At a high SNR, the performance with this ordering is better than the detector using the SAI-SO. For the PA-SIC detector, here, we only choose three branches with three different SOs—SAI-SO, DP-SO, and one random SO. It can be observed that the PA-SIC provides a gain of about 2 dB over that of the SIC receiver. The MLSE decoder gives the best performance; however, at  $\text{BER} = 10^{-4}$ , there is only 1-dB loss using the PA-SIC with  $K = 3$ . Note that the complexity of the MLSE is very high. We also include the results that are obtained by channel estimation, as shown in Fig. 2(b), and thus, some estimation errors are introduced. We can observe that the performance of all detectors degrades due to the channel estimation errors: around 2-dB loss can be observed in comparison with the corresponding curves in Fig. 2(a). However, the conclusion is the same as the case with perfect channel estimation.

Fig. 3 shows the simulation results for the PA-SIC with perfect channel estimation in the doubly selective fading environment. Here,

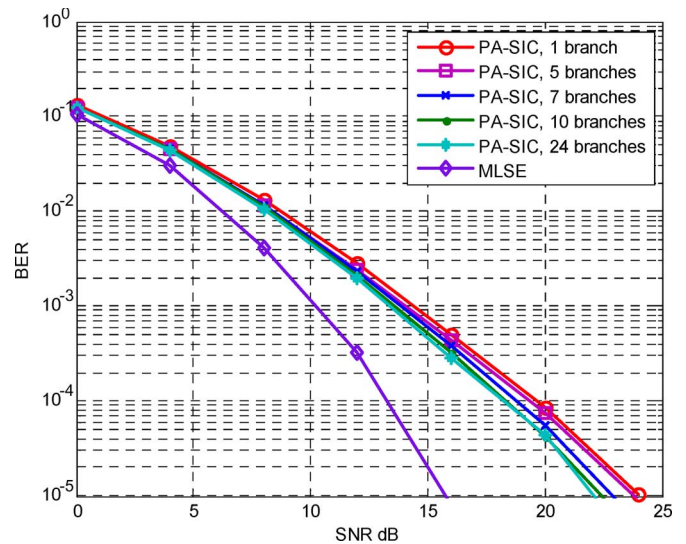


Fig. 3. PA-SIC. Doubly selective fading channels; length of the frame = 4, taps = 2,  $F_d T_s = 0.0093$ ,  $k = 1, 5, 7, 10$ , and 24; BPSK.

we focus on the optimal PA-SIC that tests all decoding possibilities and presents an exhaustive search problem. For simplicity, we set the frame length equal to four and the number of taps to two. Note that because of the exponential complexity of the exhaustive search, we had to focus on a very small frame length. Several different SIC SOs are used in parallel.

From the results, we observe that as the number of SO branches increases (all possibilities:  $4! = 24$ ), performance begins to converge, which implies that only a certain number of SIC branches will be required to provide good performance. Hence, a tradeoff between complexity and performance can be established. Note that for other numbers of taps and frame lengths, we can also come to the same conclusion. Comparison of Figs. 2 and 3 also shows that the performance of the SIC and PA-SIC detectors improves with frame length since the Gaussian approximation becomes more reliable.

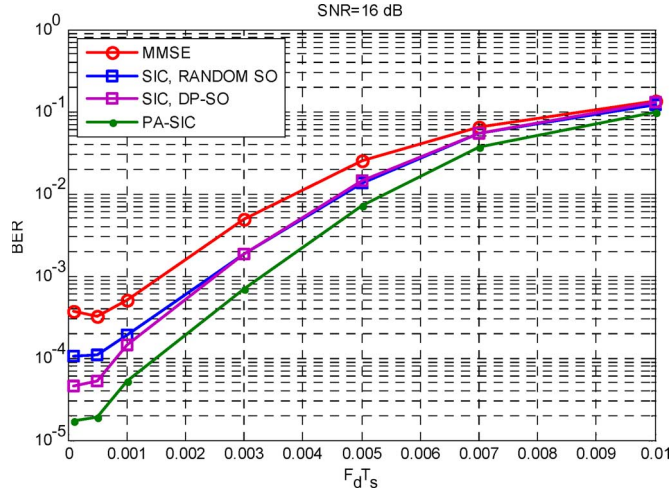


Fig. 4. SIC and PA-SIC. Doubly selective fading channels; length of the frame = 4, taps = 2,  $k = 24$ , with channel estimation; BPSK; SNR = 16 dB.

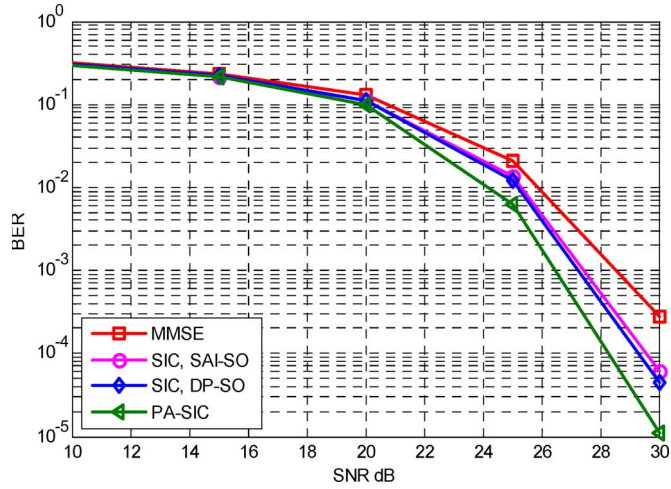


Fig. 5. SIC. Doubly selective fading channels; length of the frame = 64, taps = 3,  $F_d T_s = 0.0093$ , 16-QAM. Channel estimation.

In Fig. 4, simulation results are plotted over doubly selective fading channels against Doppler shift at SNR = 16 dB, and LS channel estimation is performed using training sequences at the receiver end. The results show that the SIC and the PA-SIC (all possibilities:  $4! = 24$ ) can provide relatively better performance than the MMSE for  $F_d T_s$  less than 0.01. We also note from the comparison of Fig. 4 that at low  $F_d T_s$  (up to 0.005), a higher SNR can lead to much better performance. However, as  $F_d T_s$  increases, there will be more channel estimation errors introduced so that the performance gains obtained in Fig. 4 are no longer clear.

Last, to show that our SIC and PA-SIC are not limited to BPSK constellations, in Fig. 5, we apply 16-QAM to generate a 4-b/s/Hz transmission rate. The simulations are obtained under doubly selective fading channels with  $F_d T_s = 0.0093$ , and channel estimation is employed. From the results, we can come to the same conclusion that the SIC can give better performance than the MMSE, and SO is useful to obtain better performance. The PA-SIC provides much better performance than the SIC due to the soft combining of the output from each SIC branch.

## V. CONCLUSION

In this paper, we propose two schemes for the TR-STBCs to combat frequency-selective fading. In relatively time-invariant environments,

the SIC can be used to recover the original data with promising performance and very low complexity. For doubly selective fading channels, we further parallel-concatenate a certain number of SIC detectors with different signal decoding sequences and combine the soft output of each individual SIC. Simulation shows that the PA-SIC is very robust and can provide much better performance than the SIC and the MMSE, and the tradeoff between computational complexity and system performance can be easily realized by adjusting the number of SIC subbranches.

## APPENDIX

In this section, we aim to simplify the matrix inversion term. For (18), rewriting the multiplication term in  $\exp(\cdot)$ , we can obtain

$$\begin{aligned} (\tilde{\mathbf{y}} - \mathbf{j}_k s_k)^H \Lambda_k^{-1} (\tilde{\mathbf{y}} - \mathbf{j}_k s_k) \\ = \tilde{\mathbf{y}}^H \Lambda_k^{-1} \tilde{\mathbf{y}} + |s_k|^2 \mathbf{j}_k^H \Lambda_k^{-1} \mathbf{j}_k - 2\text{Re}(\tilde{\mathbf{y}}^H \Lambda_k^{-1} \mathbf{j}_k s_k). \end{aligned}$$

The first term is a constant, and thus, we do not need to consider it in probability computation, such that we can concentrate on the term that needs matrix inversion, i.e.,

$$\begin{aligned} \Lambda_k^{-1} &= (\mathbf{J}_{k+1,2N}^H \mathbf{J}_{k+1,2N} |\bar{s}|^2 + \sigma^2 \mathbf{H}^H \mathbf{I})^{-1} \\ &= \frac{1}{\sigma^2 \mathbf{H}^H} - \frac{\mathbf{J}_{k+1,2N}^H \mathbf{J}_{k+1,2N} |\bar{s}|^2}{\sigma^2 |\bar{s}|^2 \mathbf{J}_{k+1,2N}^H \mathbf{J}_{k+1,2N} \mathbf{H}^H + \sigma^4 \mathbf{H}^2 \mathbf{H}} \end{aligned}$$

where  $\mathbf{J}_{k+1,2N}^H \mathbf{J}_{k+1,2N}$  can be initially obtained by calculating  $\mathbf{H}^H \mathbf{H}$  and storing it in the memory. As a result, the matrix inversion is no longer required, and the term in  $\exp(\cdot)$  of (18) can be represented as

$$(\tilde{\mathbf{y}} - \mathbf{J}_k s_k)^H \Lambda_k^{-1} (\tilde{\mathbf{y}} - \mathbf{J}_k s_k) \propto |s_k|^2 \mathbf{j}_k^H \Lambda_k^{-1} \mathbf{j}_k - 2\text{Re}(\tilde{\mathbf{y}}^H \Lambda_k^{-1} \mathbf{j}_k s_k).$$

## REFERENCES

- [1] G. J. Foschini and M. J. Gans, "On limits of wireless communications in a fading environment when using multiple antennas," *Wirel. Pers. Commun.*, vol. 6, no. 3, pp. 311–335, Mar. 1998.
- [2] I. E. Telatar, *Capacity of Multi-Antenna Gaussian Channels*, Jun. 1995. AT&T Bell Labs Intern. Rep.
- [3] I. E. Telatar, "Capacity of multi-antenna Gaussian channels," *Eur. Trans. Telecommun.*, vol. 10, no. 6, pp. 585–595, Nov./Dec. 1999.
- [4] G. J. Foschini, "Layered space-time architecture for wireless communication in a fading environment when using multi-element antennas," *Bell Labs Tech. J.*, vol. 1, no. 2, pp. 41–59, Autumn 1996.
- [5] S. M. Alamouti, "A simple transmit diversity technique for wireless communications," *IEEE J. Sel. Areas Commun.*, vol. 16, no. 8, pp. 1451–1458, Oct. 1998.
- [6] V. Tarokh, H. Jafarkhani, and A. R. Calderbank, "Space-time block coding for wireless communications: Performance results," *IEEE J. Sel. Areas Commun.*, vol. 17, no. 3, pp. 451–460, Mar. 1999.
- [7] V. Tarokh, H. Jafarkhani, and A. R. Calderbank, "Space-time block codes from orthogonal designs," *IEEE Trans. Inf. Theory*, vol. 45, no. 5, pp. 1456–1467, Jul. 1999.
- [8] E. Lindskog and A. Paulraj, "A transmit diversity scheme for channels with interference," in *Proc. IEEE ICC*, New Orleans, LA, Jun. 2000, vol. 1, pp. 307–311.
- [9] Z. Liu, G. Giannakis, A. Scaglione, and S. Barbarossa, "Decoding and equalization of unknown multipath channels based on block precoding and transmit-antenna diversity," in *Proc. 33rd Asilomar Conf. Signals, Syst., Comput.*, Oct. 1999, vol. 2, pp. 1557–1561.
- [10] H. Bolcskei and A. J. Paulraj, "Space-frequency coded broadband OFDM systems," in *Proc. IEEE WCNC*, Chicago, IL, Sep. 2000, pp. 1–6.
- [11] N. Al-Dhahir, "Single-carrier frequency-domain equalization for space-time block-coded transmissions over frequency-selective fading channels," *IEEE Commun. Lett.*, vol. 5, no. 7, pp. 304–306, Jul. 2000.
- [12] S. Zhou and G. Giannakis, "Single-carrier space-time block-coded transmissions over frequency-selective fading channels," *IEEE Trans. Inf. Theory*, vol. 49, no. 1, pp. 164–179, Jan. 2003.

- [13] N. Al-Dhahir, "Overview and comparison of equation schemes for space-time coded signals with application to EDGE," *IEEE Trans. Signal Process.*, vol. 50, no. 10, pp. 2477–2488, Oct. 2002.
- [14] S. Geirhofer, L. Tong, and A. Scaglione, "Time-reversal space-time coding for doubly-selective channels," in *Proc. IEEE WCNC*, Las Vegas, NV, 2006, pp. 1638–1643.
- [15] J. Luo, K. R. Pattipati, P. K. Willett, and F. Hasegawa, "Near-optimal multiuser detection in synchronous CDMA using probabilistic data association," *IEEE Commun. Lett.*, vol. 5, no. 9, pp. 361–363, Sep. 2001.
- [16] Y. Jia, C. Andrieu, R. J. Piechocki, and M. Sandell, "Gaussian approximation based mixture reduction for near optimum detection in MIMO systems," *IEEE Commun. Lett.*, vol. 9, no. 11, pp. 997–999, Nov. 2005.
- [17] P. W. Wolniansky, G. J. Foschini, G. D. Golden, and R. A. Valenzuela, "V-BLAST: An architecture for realising very high data rates over the rich-scattering wireless channel," in *Proc. ISSSE*, Pisa, Italy, Sep. 1998.
- [18] G. Barriac and U. Madhow, "PASIC: A new paradigm for low-complexity multiuser detection," in *Proc. Conf. Inf. Sci. Syst.*, Mar. 21–23, 2001.
- [19] G. H. Golub and C. D. Loan, *Matrix Computations*. Baltimore, MD: Johns Hopkins Univ. Press, 1996.

## Frequency Domain Equalization and Interference Cancellation for TD-SCDMA Downlink in Fast Time-Varying Environments

Yuhong Wang, Ying-Chang Liang, and Wing Seng Leon

**Abstract**—In time division synchronous code division multiple access downlink, one computationally efficient receiver for fast time-varying environments is the subblock processing receiver, which utilizes overlap-save fast Fourier transform. In this paper, we first analyze the interferences involved with the subblock processing method proposed by Held and Kerroum and then propose a new subblock processing receiver for fast time-varying channels. The proposed receiver consists of two stages. In the first stage, the entire received chip block is partitioned into overlapping subblocks and they are individually equalized and despread. We then artificially generate the interferences caused by adjacent blocks and the unwanted chip interference within the same subblock and eliminate them from the received data signals. Then, a second subblock processing is performed to detect the transmitted symbols. A practical channel estimator is also introduced to be used with the proposed receiver. Simulation results have shown that the proposed receiver provides a significant performance improvement as compared with the conventional subblock processing method.

**Index Terms**—Frequency domain equalization (FDE), interference cancellation, iterative algorithms, time division synchronous code division multiple access (TD-SCDMA).

### I. INTRODUCTION

The third generation cellular communication systems are based on code division multiple access (CDMA) technology due to its capability to support flexible and high rate services. Although the RAKE receiver performs maximal-ratio combining by capturing the energies from the various multipath components of the channel, it is not able to restore the orthogonality of the spreading codes, which is destroyed

Manuscript received January 13, 2005; revised October 6, 2005, July 14, 2006, January 9, 2007, and May 1, 2007. The review of this paper was coordinated by Dr. Y.-P. E. Wang.

Y. Wang is with ST Electronics (Satcom & Sensor Systems) Pte Ltd., Singapore 609602 (e-mail: wangyh@stee.stengg.com).

Y.-C. Liang and W. S. Leon are with the Institute for Infocomm Research, Singapore 119613 (e-mail: ycliang@i2r.a-star.edu.sg; wsleon@i2r.a-star.edu.sg).

Digital Object Identifier 10.1109/TVT.2007.905259

after transmission over time dispersive multipath channels. Thus, the multiple access interference (MAI) and interfinger interference (IFI) ultimately lead to an irreducible bit error rate (BER) floor if the RAKE receiver is used. Therefore, chip-level block-based equalization receivers for CDMA systems have been proposed to restore the orthogonality of the spreading codes and thereby alleviating the MAI and IFI [1]–[7].

In this paper, we consider the time division synchronous code division multiple access (TD-SCDMA) system, which has been adopted by the Third Generation Partnership Project as the low chip rate version of the Universal Mobile Telecommunications System time division duplex. For TD-SCDMA, each frame interval is 10 ms and it contains two subframes. Each subframe consists of seven slots [11], [12]. Each slot contains two data bearing blocks, each with 352 chips. The midamble between the two data bearing blocks, containing 144 chips, is designed for the purpose of channel estimation. One direct method is to estimate the channel coefficients using the midamble and then equalizing the two data blocks. This approach assumes that the channel is essentially static over the entire slot. For time-varying environments, an alternative solution is to employ subblock processing as proposed in [1], which estimates the channel estimates for each subblock, and the channel can be considered stationary, and thus, block equalization can be applied. However, subblock processing proposed in [1] introduces interference between the subblocks and interference due to the edge effect within each subblock because of the subblock dividing, which leads to an irreducible BER floor.

In this paper, we propose a novel subblock processing receiver for TD-SCDMA downlink in fast fading environment. The new receiver consists of two stages. The first stage is similar to the conventional subblock processing equalizer [1]. Using the decisions derived from the first stage, the receiver then artificially generates the estimates of the interferences, which are then eliminated from the received data chip block. A second subblock processing is finally performed to detect the transmitted symbols. We also present a practical channel estimation method to be used with the proposed receiver.

This paper is organized as follows. In Section II, the downlink transmission model of TD-SCDMA is described, and the conventional subblock processing method is introduced. In Section III, the proposed receiver and channel estimator are presented. In this section, the complexity of the proposed receiver is also compared with that of the conventional receiver. Computer simulation results are given in Section IV for various channel environments. Finally, we conclude this paper in Section V.

### II. SYSTEM MODEL AND CONVENTIONAL SUBBLOCK PROCESSING RECEIVER

In this section, we will briefly describe the TD-SCDMA downlink system and introduce the conventional subblock processing receiver.

#### A. Channel Model

We consider a single cell TD-SCDMA downlink with processing gain  $Q$  and  $K$  active users. The data symbols designed for all  $K$  active users are synchronously and simultaneously transmitted from the base station to the mobile units over the same downlink channel. Within each time slot, there are two data bearing blocks. For each block,  $N$  data symbols are transmitted for each of the  $K$  users. The data symbols may be written as

$$\mathbf{d}^{(k)} = \left[ d_1^{(k)}, d_2^{(k)}, \dots, d_N^{(k)} \right]^T \quad (1)$$